ELSEVIER

Polymer 41 (2000) 6913–6918

polymer

# Residual stress and microstructures of aromatic polyimide with different imidization processes

T. Nishino, M. Kotera, N. Inayoshi, N. Miki, K. Nakamae*

*Department of Chemical Science and Engineering, Kobe University, Rokko, Nada, Kobe 657-8501, Japan*

Received 8 September 1999; accepted 5 December 1999

**Abstract**

Processing of polyimide (PI) from precursor polyamic acid (PAA) solution involves simultaneous imidization, evaporation of solvent and crystallization, so imidization process influences the final properties of PI. The residual stress at the interface between the most popular PI (PMDA–ODA) and the aluminum substrate was measured by X-ray diffraction method and the relationship between the microstructure and the mechanical properties was investigated for PI with different imidization processes. The residual stress and the mechanical properties of PI depend on the imidization process. The skeletal structure is suggested to be changed by the amount of residual solvent during imidization process, which brings the difference in the residual stress. © 2000 Elsevier Science Ltd. All rights reserved.

*Keywords*: Polyimide; Residual stress; X-ray diffraction

## 1. Introduction

Aromatic polyimides (PI) have excellent thermal stability, good mechanical properties and low electric constant, hence they are widely used as microelectronics devices. When PI films are used as flexible printed circuitry boards and interlayer dielectrics, a thermal expansion mismatch between the film and the metal wiring causes residual stress at the interface through cooling down from the curing temperature to room temperature. This thermal stress might cause adhesion failure between the PI film and the metal [1]. Thus, in order to satisfy the demand of high-performance for materials, reducing of the residual stress has been the most important problem. Several methods have been reported to detect the residual stress by using a strain gauge [2–4], a bimetal [5,6], a photoelasticity [7], a layer removal procedure [8] and so on. Among them, we have proposed a novel technique, X-ray diffraction method, in which the microscopic deformation of the crystal lattice was detected nondestructively. In the previous papers [9,10], this method was successfully applied to detect the residual stress of epoxy resin–metal interfaces.

PI films are generally prepared from precursor polyamic acid (PAA) solution by casting followed by thermal curing. The thermal curing process involves the simultaneous cyclization with dehydration, evaporation of solvent and crystallization, so it will influence the final properties of PI [11–14]. In the previous paper [15], we manifested a glass transition temperature ($T_g$) of PAA cast from different solvent by the temperature-modulated differential scanning calorimetry. The $T_g$ value of PAA was effected by the amount of residual solvent during the imidization process.

In this study, the X-ray diffraction method was applied to detect the residual stress at the interface between the PI film and the aluminum substrate nondestructively. The effect of imidization process on the microstructures and the mechanical properties of PI were investigated.

## 2. Experimental

### 2.1. Sample preparation

Polyamic acid (PAA) precursor was prepared by the conventional ring-opening polyaddition reaction [16]. Pyromellitic dianhydride (PMDA) was added dividedly several times to a three-neck flask without precipitation to *N*-methyl-2-pyrrolidone (NMP) in which oxydianiline (ODA) was previously dissolved. After the mixture was stirred for 1 h under dry nitrogen gas flow, PMDA–ODA PAA 13.8 wt% in NMP solution was synthesized. The adherend used is aluminum (Al) plate (50 × 70 × thickness

* Corresponding author. Tel.: + 81-78-803-6191; fax: + 81-78-803-6205.

*E-mail address:* nakamae@cx.kobe-u.ac.jp (K. Nakamae).

0032-3861/00/$ - see front matter © 2000 Elsevier Science Ltd. All rights reserved.
PII: S0032-3861(00)00002-1

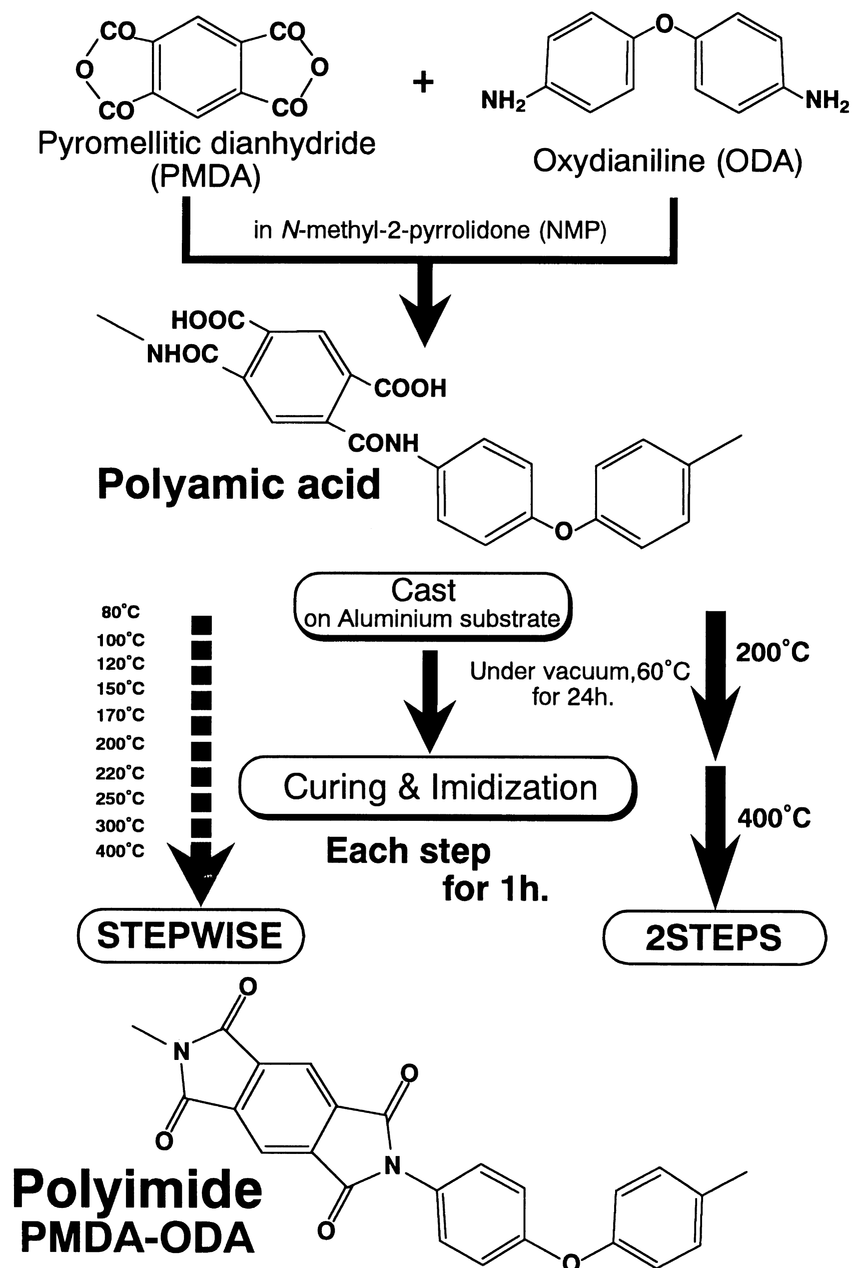


Fig. 1. Experimental procedure for the sample preparation of PMDA–ODA polyimide.

4 mm). In order to enhance the adhesion, the Al plate was pre-treated with chromic acid (JIS K 6848).

Fig. 1 shows the experimental procedure for the sample preparation. PMDA–ODA PAA solution was cast on the Al plate followed by drying at 60°C for 24 h under vacuum. After that, in this study, PAA was cured with two different ways. In one treatment (STEPWISE), PAA was cured at 80, 100, 120, 150, 170, 200, 220, 250, 300 and finally at 400°C successively for 1 h at each step. In the other treatment (2STEPS), PAA was cured at 200°C for 1 h first and then 400°C for another 1 h. Finally, PMDA–ODA PI, the most popular so-called Kapton type PI, was obtained in both ways. Final thickness of the PI film was about 100 μm. The shape and dimensions of the specimen for the residual stress measurements are shown in Fig. 2.

Fig. 3 shows the infrared spectra of STEPWISE sample before and after thermal curing. A Fourier transform infrared (FT-IR) spectrophotometer (Shimadzu FT-IR 4200) was used at a resolution of 2 $cm^{-1}$, and 10 accumulations. The absorption at 1550 $cm^{-1}$ (amide I:CNH vibration) disappeared after the curing, on the other hand, the absorption at 1380 $cm^{-1}$ (imide II:C–N stretching vibration) and that at 730$cm^{-1}$ (imide IV:bending vibrations of cyclic C=O) appeared [17]. These indicate that the precursor PAA was converted into PI by thermal curing up to 400°C. The conversion to PI during the thermal imidization at

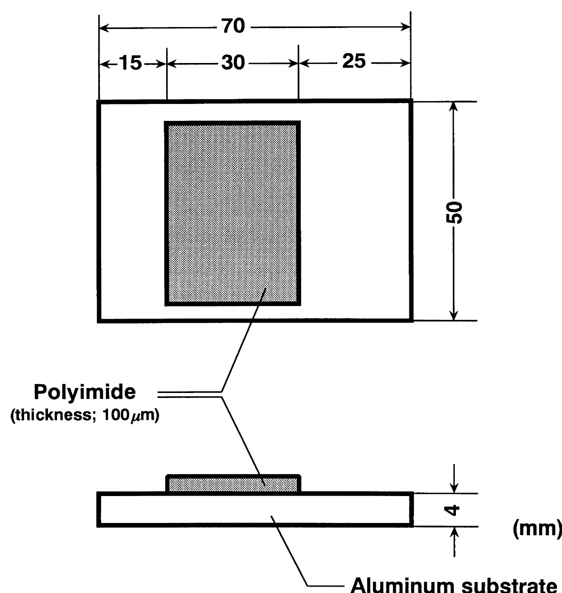


Fig. 2. Shape dimension of the specimen for the residual stress measurements.

temperature $T$ was determined by the following equation:

$$\text{Conversion to PI}(\%) = \{(D_{1380\ \mathrm{cm}^{-1}}/D_{1500\ \mathrm{cm}^{-1}})_T/(D_{1380\ \mathrm{cm}^{-1}}/D_{1500\ \mathrm{cm}^{-1}})_{400°\mathrm{C}}\} \times 100 \tag{1}$$

where, $D$ is the optical density of each absorption. The absorption band at 1500 $\mathrm{cm}^{-1}$ (C–C stretching of the *p*-substituted benzene) is selected as an internal standard.

The specimen density was measured by a floatation method (chlorobenzene–carbon tetrachloride system) at 30°C. Specimen modulus ($Y$) was measured by a tensile tester (Shimadzu AUTOGRAPH AGS-1 kND) at room temperature. The original length of the specimen was 20 mm and the cross head speed was 2 mm/min, respectively.

A linear thermal expansion coefficient ($\alpha_f$) was measured by a thermal mechanical analyzer (Seiko Instruments Inc. TMA/SS120CU) from −100 to 400°C. A heating rate of 10°C/min, a original length of 15 mm and a tensile load of 1 MPa were employed.

Dynamic modulus ($E'$) was measured by a dynamic mechanical analyzer (ITK Co. Ltd DVA-220S) from −50 to 400°C. A heating rate of 6°C/min, a original length of 10 mm and a frequency of 10 Hz were employed.

The amount of residual solvent was estimated by a thermogravimeter (Seiko Instruments Inc. TG/DTA220U) on each thermal step. Total weight loss during the heating process includes both the evaporation of solvent and the dehydration with cyclization. The amount of the dehydration could be calculated from the conversion to PI from FT-IR. Thus, by subtracting the amount of dehydration from the total weight loss, the amount of residual solvent during the heating process was evaluated.

### 2.2. Measurement of residual stress by X-ray diffraction

Fig. 4 shows the principle of the measurement of residual stress by X-ray diffraction method. A cured specimen on Al substrate was set on an X-ray diffractometer (Rigaku Denki RAD-B system) operated at a tube voltage of 40 kV, a tube current of 20 mA for CuK$\alpha_1$ radiation, with a divergence slit width of 0.5°. PI was cast and cured at high temperature as described above, which adhered strongly to the Al substrate. At a cooling process to room temperature after the curing, the crystal lattice of the Al would be strained because of the difference in the thermal expansion between the PI film and the substrate. The Al crystal is a cubic system ($a =$ 4.0497 Å at 23°C) with a thermal expansion coefficient $\alpha_s$ of $2.386 \times 10^{-5}\ \mathrm{K}^{-1}$. The strain $\epsilon$ of Al crystal, which was

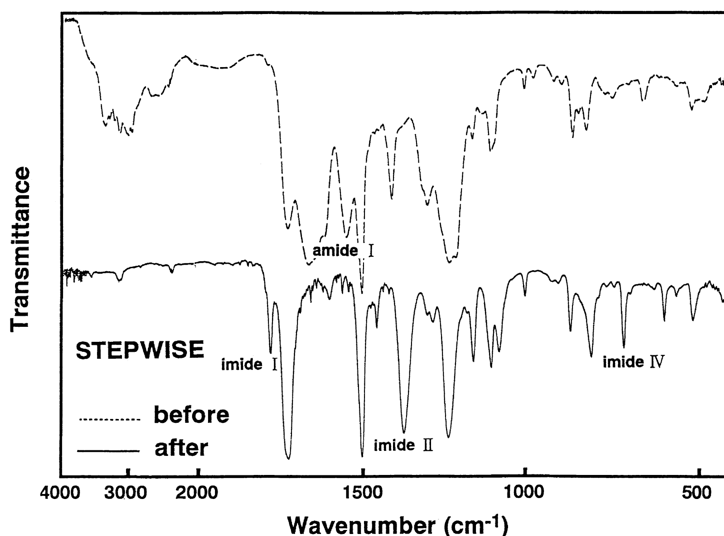


Fig. 3. Infrared spectra of PMDA–ODA polyamic acid (STEPWISE) before and after thermal curing.

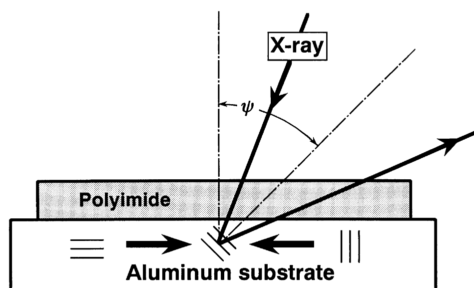


Fig. 4. Schematic representation for the residual stress measurement by X-ray diffraction.

detected as a shift of the diffraction angle $2\theta$ by Bragg's equation, could be measured by the following equation:

$$\epsilon = (d - d_0)/d_0 \tag{2}$$

where, $d_0$ is the initial lattice spacing for the (422) plane ($2\theta = 137.5°$ for $CuK\alpha_1$) of the Al crystal, and $d$ is that after the curing. Temperature was monitored by contacting a thermocouple to the Al substrate from the back side of the PI film, and the lattice spacings were converted into values at 23°C.

When $\epsilon$ is measured with a symmetric reflection geometry, $\epsilon$ is the strain in the direction perpendicular to the Al substrate. In order to get information about the directionality of the residual stress, the $\sin^2\psi$ method was employed. In this method, when the sample is subjected to a uniaxial stress, the relationship between the strain $\epsilon_\psi$ and the inclination angle $\psi$ can be expressed with the following equation [18]:

$$\epsilon_\psi = \{(1 + \nu)\sigma/E\}\sin^2 \psi - (\nu/E)\sigma \tag{3}$$

where, $\nu$ is Poisson's ratio of Al crystal (0.33), $E$ is the elastic modulus of Al crystal (75.5 GPa), and $\sigma$ is the residual stress. From the slope between $\epsilon_\psi$ and $\sin^2\psi$ plots, we can get information about the value and the direction of the residual stress.

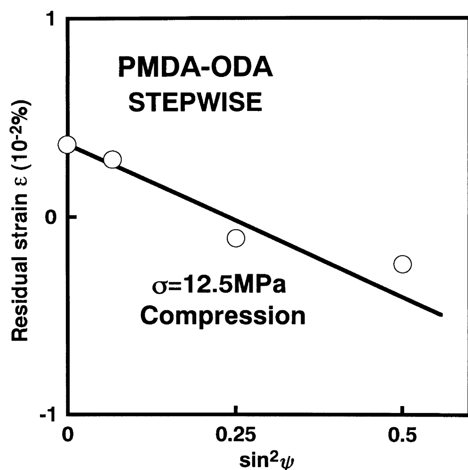


Fig. 5. Relationship between the residual strain $\epsilon_\psi$ of Al substrate and $\sin^2\psi$ for PMDA–ODA polyimide (STEPWISE) on the Al substrate.

## 3. Results and discussion

Fig. 5 shows the relationship between the residual strain $\epsilon_\psi$ of Al substrate and $\sin^2\psi$ for PI cured with STEPWISE sample on the Al substrate. The plots could be expressed with a straight line with a minus gradient, where $\epsilon > 0$ at $\psi = 0°$ (in the direction perpendicular to the substrate surface), while $\epsilon < 0$ at $\psi = 90°$ (in the direction parallel to the substrate surface). A minus gradient indicates that the Al substrate was subjected to a uniaxial compressive stress of 12.5 MPa for STEPWISE sample. When the specimen was cooled down to room temperature from the curing temperature (400°C), the PI film and the Al substrate would shrink, however, a linear thermal expansion coefficient ($\alpha_f$) of PI is far larger than that ($\alpha_s$) of Al crystal, so the stress would remain at the interface.

This thermal stress $\sigma$ can be expressed with the following equation [19]:

$$\sigma_{calcd} = \int_{r.t.}^{400°C} \frac{Y}{1 - \nu_f}(\alpha_s - \alpha_f)\, dT \tag{4}$$

where, $\nu_f$ is the Poisson's ratio of the film, here assumed to be 0.30. This equation reveals that the residual stress is the function of Young's modulus ($Y$) and the thermal expansion coefficient ($\alpha_f$) of the film.

Fig. 6 shows the temperature dependence of the dynamic storage modulus $E'$ and the $\alpha_f$ value of PI cured with STEPWISE sample. The $\alpha_s$ value of Al is also superposed on the figure with filled circles. On increasing the temperature, $E'$ value decreased and $\alpha_f$ value increased linearly. Based on these data, the residual stress was calculated with Eq. (4).

Table 1 shows the observed and the calculated residual stresses and some characteristics of PI with different imidization processes. The residual stress of 2STEPS sample was about 1.2 times higher than that of STEPWISE sample, which coincided with the calculated values within the experimental error. Accordingly, in spite of the same final chemical structure of PMDA–ODA PI, the residual stress could be reduced by changing the imidization processes. Specimen modulus ($Y$) of 2STEPS sample showed 1.2 times higher than that of STEPWISE sample. This difference in specimen modulus is considered to be a key factor for the difference of residual stress of PI by changing the imidization process.

Fig. 7 shows a schematic representation of the skeletal structure of PMDA–ODA PI, where a fiber identity period is defined as shown in the figure. PMDA–ODA PI possesses rigid structure because the molecular chain is composed of phenyl and imide rings, so the change of the fiber identity period should be brought about only by the change in the bonding angle ($\theta$) at the ether linkage.

Table 2 shows the fiber identity period measured from the

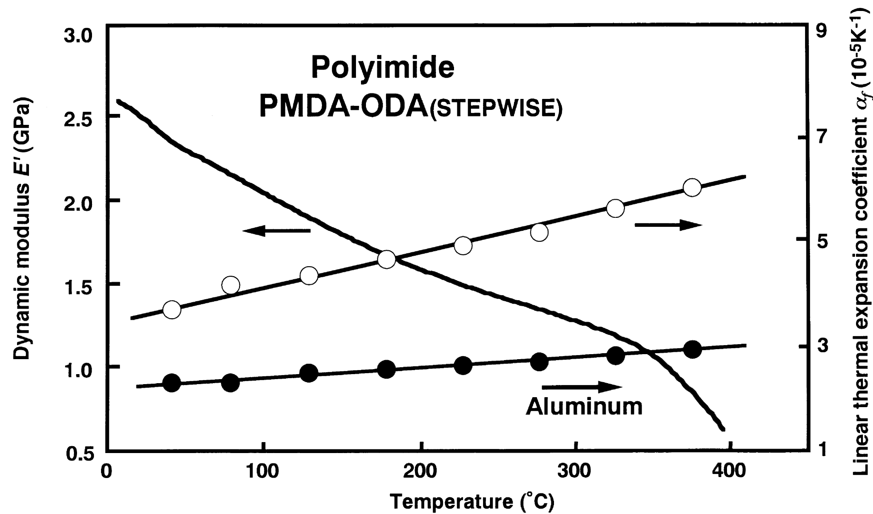


Fig. 6. Temperature dependences of the dynamic modulus $E'$ and the linear thermal expansion coefficient $\alpha_f$ value of PMDA–ODA polyimide (STEPWISE) and Al.

lattice spacing of the (004) plane and the $\theta$ value at the ether linkage calculated from it. The fiber identity period of 2STEPS sample is longer, and $\theta$ is larger than that of the STEPWISE sample. The experimental error in measuring the peak position was evaluated to be generally less than $\pm 0.004°$ in the diffraction angle $2\theta$, which corresponds to the change in the lattice spacing of 0.01 Å for the (004) plane. Thus the difference in the fiber identity period is far above the experimental error. Accordingly, it follows from the fiber identity period that the skeleton of the STEPWISE sample is more contracted compared with that of the 2STEPS sample. This also reflects the elastic modulus ($E_l$) of the crystalline regions of PI. The $E_l$ value of the STEPWISE sample is 9.1 GPa and that of the 2STEP sample is 15 GPa in the direction parallel to the chain axis [20]. Thus, more contracted structure is considered to bring the low $E_l$ value and the low specimen modulus for the STEPWISE sample, and this is considered to be the reason for the low residual stress for the STEPWISE sample.

As described before, imidization process of PI from precursor PAA solution involves simultaneous cyclization with dehydration, evaporation of solvent and crystallization, competitively. Hence, it will also influence the final properties of PI. Next, the effect of imidization process on the skeletal structure and the mechanical properties was investigated for PI with different imidization processes.

Fig. 8 shows the relationship between the conversion to PI from PAA and the amount of residual NMP solvent. The residual solvent was completely evaporated at the final stage of thermal curing (400°C) in both cases. However, the amount of residual solvent during imidization process was different. For the STEPWISE sample, imidization seemed to progress with high residual solvent compared with the 2STEPS sample. This indicates that the STEPWISE sample was imidized with high chain mobilities due to high residual solvent, so the molecular chain of the STEPWISE sample was easy to bend at the ether linkage. Thus, PI was crystallized into thermodynamically stable state, in other words, more contracted skeletons. The residual solvent acts as a plasticizer during the imidization process. This is considered to be the reason for the low residual stress for the STEPWISE sample.

Table 1
Residual stress and some characteristics of PMDA–ODA polyimide with different imidization processes

| | STEPWISE | 2STEPS |
|---|---|---|
| Residual stress $\sigma$ (MPa) | | |
| X-ray diffraction | 12.5 | 15.4 |
| Calculated | 11.6 | 15.6 |
| Specimen modulus $Y$ (GPa)[a] | 2.0 | 2.4 |
| Density (g/cm$^3$)[b] | 1.41 | 1.43 |

[a] At 23°C.
[b] At 30°C.

## 4. Conclusions

The residual stress at the adhered interface between PMDA–ODA PI film and Al substrate was investigated by X-ray diffraction method. The residual stress of the STEPWISE sample was lower than that of the 2STEPS sample. This result was reflected by the difference of the

Table 2
Fiber identity period for the (004) plane and the bonding angle $\theta$ at the ether linkage of PMDA–ODA polyimide with different imidization processes

| | STEPWISE | 2STEPS |
|---|---|---|
| Fiber identity period (Å) | 32.18 | 32.40 |
| Bonding angle $\theta$ (°) | 124.8 | 126.2 |

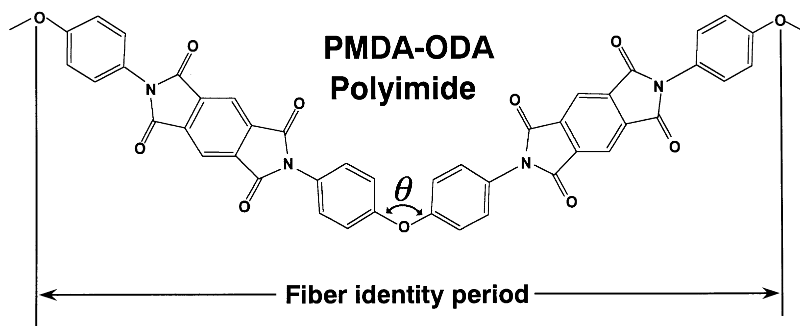


Fig. 7. Schematic representation of the skeletal structure of PMDA–ODA polyimide.

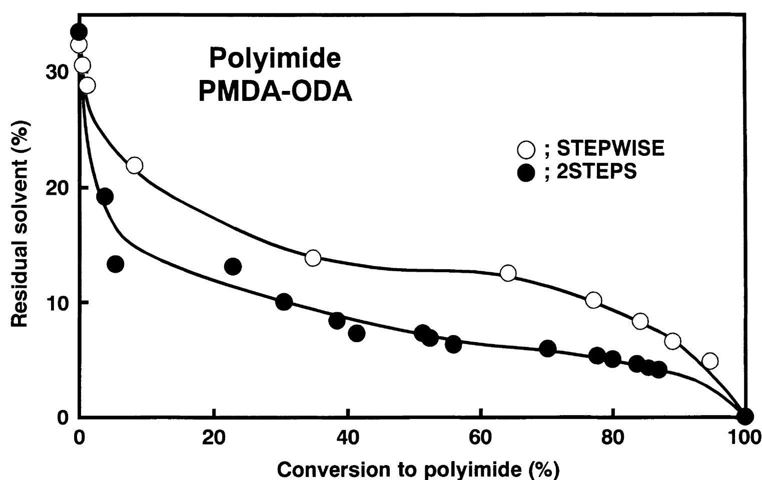


Fig. 8. Relationship between the conversion to polyimide from polyamic acid and the amount of residual solvent.

specimen modulus of PI by different imidization processes. High residual solvent during imidization process gave a high molecular mobility, which brought PI molecules more contracted skeletal structure at the ether linkage. This is considered to bring the low specimen modulus, which resulted in the low residual stress for STEPWISE.

According to these results, the selection of imidization condition (thermal treatment or evaporation speed of solvent) brought the different skeletal structure of PI PMDA–ODA. Thus it effected the final mechanical properties of PI. Accordingly, controlling of the imidization processes will bring high performance such as low residual stress or high elastic modulus to PI.

## References

[1] Ree M, Chu CW, Goldberg MJ. J Appl Phys 1994;75:1410.
[2] Shimbo M, Ochi M, Shigeta Y. J Appl Polym Sci 1981;26:2265.
[3] Shimbo M, Yoshida T, Minamoto M. Kobunshi Ronbunshu 1983;40:1.
[4] Shimbo M, Ochi M, Arai K. J Coat Technol 1984;56:45.
[5] Kosuge N. J Adhesion Soc (Jpn) 1971;7:170.
[6] Inoue Y, Kobatake Y. Kolloid-Z 1958;159:18.
[7] Theocaris PS, Paipetis SA. J Strain Anal 1973;8:286.
[8] Srivastava AK, White JR. J Appl Polym Sci 1984;29:2155.
[9] Nakamae K, Nishino T, Xu Airu, Matsumoto T, Miyamoto T. J Appl Polym Sci 1990;26:2265.
[10] Nishino T, Xu Airu, Matsumoto T, Matsumoto K, Nakamae K. J Appl Polym Sci 1992;45:1239.
[11] Kim HT, Park JK. Polym J 1997;29:1002.
[12] Ojeda JR, Mobley J, Martin DC. J Polym Sci Part B: Polym Phys 1995;33:559.
[13] Miwa T, Okabe Y, Ishida M. Polymer 1997;38:4945.
[14] Stoffel NC, Kramer EJ, Volksen W, Russell TP. Polymer 1993; 34:4524.
[15] Kotera M, Nishino T, Nakamae K. Polymer 2000; (in press).
[16] Sroog CE, Endrey AL, Abramo SV, Berr CE, Edwards WM, Olivier KL. J Polym Sci Part A 1965;3:1373.
[17] Pryde CA. J Polym Sci Part A: Polym Chem 1989;27:711.
[18] Cullity BD. Elements of X-ray diffraction. 2nd ed.. Reading, MA: Addison-Wesley, 1980 (chap. 17).
[19] Coburn JC, Pottiger MT, Noe SC, Senturia SD. J Polym Sci Part B: Polym Phys 1994;32:1271.
[20] Nishino T, Miki N, Mitsuoka Y, Nakamae K. Polym Prepr Jpn 1995;44:2947.